



Research Article

## Mechanical characterization of alumina and graphite dual particulates reinforced hybrid aluminum alloy (Al2219) matrix composites

ShivaPrakash S<sup>1,a</sup>, Santosh Kumar<sup>2,b</sup>, Naveen Kumar B K<sup>3,c</sup>, Madeva Nagaral<sup>\*4,d</sup>, Narasimha Marakal<sup>5,e</sup>, V Auardj<sup>6,f</sup>, Manjunatha T H<sup>7,g</sup>, Dileep B. P<sup>8,h</sup>

<sup>1</sup>Department of Mechanical Engineering, New Horizon College of Engineering, Bangalore-560103, India

<sup>2</sup>Department of Industrial and Production Engineering, The National Institute of Engineering, India

<sup>3</sup>Department of Mechanical Engineering, M S Ramaiah Institute of Technology, Bengaluru, India

<sup>4</sup>Aircraft Research and Design Centre, Hindustan Aeronautics Limited, Bangalore-560037, Karnataka, India

<sup>5</sup>Department of Mechanical Engineering, Nitte (Deemed to be University) NMAM Institute of Technology, Nitte, Karkala, Udupi-574110, Karnataka, India

<sup>6</sup>Department of Mechanical Engineering, Siddaganga Institute of Technology, Tumkur-572103, India

<sup>7</sup>Department of Mechanical Engineering, Ballari Institute of Technology and Management, Ballari-583104, Karnataka, India

<sup>8</sup>Department of Mechanical Engineering, Amrita School of Engineering, Amrita Vishwa Vidyapeetham, Bangalore, 560035, India

### Article Info

### Abstract

#### Article history:

Received 21 June 2024

Accepted 24 Dec 2024

#### Keywords:

Al2219 alloy;  
Graphite particles  
hybrid composite;  
Microstructure;  
Mechanical behavior

The current study involved the production of hybrid composites employing a liquid metallurgical technique, combining Al2219 alloy with Al<sub>2</sub>O<sub>3</sub> and graphite. The Al2219 alloy was employed to fabricate hybrid composites consisting of Al<sub>2</sub>O<sub>3</sub> particles, ranging from 3 to 6 weight percent, and a constant 2 weight percent of graphite particles. The generated composites underwent microstructural investigation using scanning electron microscopy (SEM) and energy-dispersive X-ray spectroscopy (EDS). The density, hardness, ultimate strength, yield strength, and elongation were determined according to ASTM standards. The SEM revealed that both graphite and Al<sub>2</sub>O<sub>3</sub> particles were uniformly distributed within the Al2219 alloy. The EDS revealed the presence of hybrid particles in the Al2219 alloy. The incorporation of dual particles into the matrix resulted in a decrease in the density of aluminium alloy composites. The incorporation of dual particles enhanced the hardness of Al2219 alloy by 22%, ultimate strength by 36.7%, and yield strength 38.5%. The EDS results indicated that the Al2219 alloy contains hybrid particles. The incorporation of dual particles into the matrix resulted in a decrease in the density of aluminium alloy composites. The unique fracture characteristics of the Al2219 alloy and its composites were further demonstrated through the use of tensile force micrographs.

© 2024 MIM Research Group. All rights reserved.

## 1. Introduction

Composites consist of many materials that possess different chemical or physical properties. Upon combining these components, a novel product is formed, exhibiting distinct features from its individual constituents [1, 2]. Usually, the material's strengthening is done on a large scale [3, 4]. In the end result, the materials are easily recognisable, but they are joined together to enhance durability, reduce weight, and

\*Corresponding author: [madeva.nagaral@gmail.com](mailto:madeva.nagaral@gmail.com)

<sup>a</sup> [orcid.org/0000-0001-5279-3522](https://orcid.org/0000-0001-5279-3522); <sup>b</sup> [orcid.org/0000-0002-6129-4466](https://orcid.org/0000-0002-6129-4466); <sup>c</sup> [orcid.org/0000-0002-3774-4551](https://orcid.org/0000-0002-3774-4551);

<sup>d</sup> [orcid.org/0000-0002-8248-7603](https://orcid.org/0000-0002-8248-7603); <sup>e</sup> [orcid.org/0000-0003-4644-7361](https://orcid.org/0000-0003-4644-7361); <sup>f</sup> [orcid.org/0000-0001-6549-6340](https://orcid.org/0000-0001-6549-6340)

DOI: <http://dx.doi.org/10.17515/resm2024.328me0621rs>

Res. Eng. Struct. Mat. Vol. x Iss. x (xxxx) xx-xx

decrease overall expenses in comparison to the conventional material. Due to its enhanced customised characteristics, the final composite material surpasses its constituent components [5, 6]. These composites are attractive alternatives due to their improved mechanical, thermal, electrical, and environmental properties. Ceramic matrix composites and metal matrix composites are in great demand for many construction applications, such as bridges, buildings, boats, swimming pools, race car parts, tanks, and innovative materials for spacecraft, aviation, and buildings [7, 8].

Typically, metal matrix composites (MMCs) consist of two phases [9, 10, 42]. The process consists of two distinct phases: the matrix phase and the reinforcing phase, with the latter often being a metal alloy. To enhance the mechanical properties of composites and achieve material qualities that cannot be achieved by a single phase, it is customary to combine the two phases [11, 12]. Researchers are intensifying attempts to develop powerful reinforcements that augment the strength of MMCs. The integration of reinforcements into the matrix phase facilitates the enhancement of attributes including wear resistance, stiffness, thermal expansion coefficient, and high-temperature conductivity. The selection of suitable filler material is essential for developing a high-quality metal matrix composite [13, 43].

Aluminum possesses several beneficial characteristics, including its low density and its ability to resist corrosion due to passivation [14]. Aluminium and aluminium alloys are essential in the aerospace and automotive industries because they are inexpensive, have a high strength-to-weight ratio, are easy to machine and shape, and are relatively lightweight. Extensive research is being carried out in this field to discover methods of enhancing the strength-to-weight ratio of aluminium alloys by incorporating exceptionally robust elements, a quality that is in high demand [15, 16]. These reinforcing materials can be utilised to modify the mechanical properties according to your requirements. Metal matrix composites (MMCs) are a recently developed material resulting from continuous research on the incorporation of reinforcing elements with base materials such as aluminum alloy [17, 18].

Raj Kumar et al. [44] and co-authors conducted a study using SEM and EDS micrographs, which distinctly demonstrated the presence of B<sub>4</sub>C and graphite particles embedded within the Al2117 matrix. The reinforcing particles significantly enhanced the hardness of the aluminium matrix. The incorporation of 3% and 6% B<sub>4</sub>C-5% graphite particles increased the hardness of the Al2117 alloy by 3.1% and 10.41%, respectively. Additionally, the ultimate tensile strength of the Al2117 alloy improved by 4.06% and 9.6% with the incorporation of 3% and 6% B<sub>4</sub>C-5% graphite particles, respectively. The use of B<sub>4</sub>C and graphite particles enhanced the yield strength of the Al2117 alloy. Nevertheless, as the concentrations of B<sub>4</sub>C and graphite particles increased, the elongation of Al2117 diminished. Fractographic analysis of tensile fracture surfaces demonstrated a combination of ductile and brittle mechanisms in both the Al2117 alloy and its composites, highlighting the intricate mechanical behaviours influenced by reinforcing particles.

Raksha et al [45] utilized Two-stage melt stirring was employed to fabricate Al2011 alloy composites containing 2 and 4wt% graphite particles (50 to 60µm). SEM micrographs demonstrated a uniform distribution of graphite particles devoid of aggregation, corroborated by EDS examination. Augmenting the graphite content led to diminished hardness, concurrently enhancing ultimate tensile and yield strengths. The incorporation of 2 and 4 wt% graphite enhanced tensile strength by 17.64% and 21.15%, respectively, while simultaneously augmenting ductility. Tensile testing revealed distinct fracture mechanisms for the Al2011 alloy and graphite composites.

Pankaj [46] and his team conducted a study. Hybrid composites were fabricated by A two-stage stir casting method was employed to integrate 4 wt.% graphite (Gr) and 12 wt.%

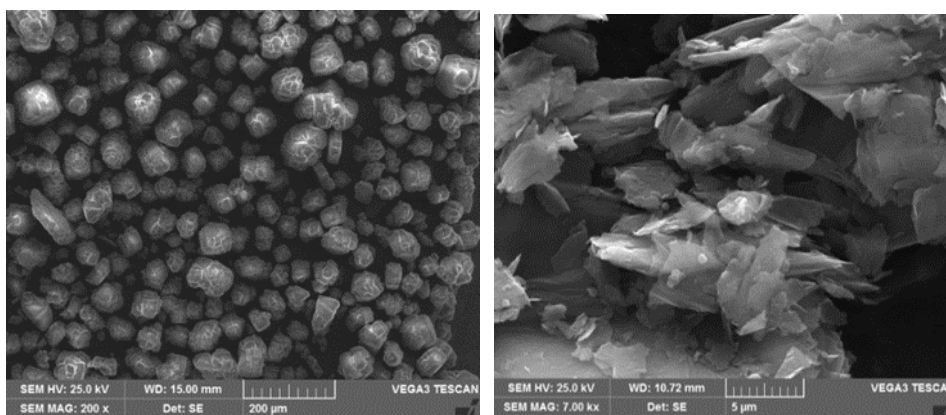
boron carbide ( $B_4C$ ) into A356 alloy, then comparing it to the standard A356 alloy. Microstructural study with SEM and EDS revealed a uniform distribution of graphite and  $B_4C$  particles throughout the matrix. The hybrid composites exhibit reduced densities owing to the lighter weights of graphite and  $B_4C$  in comparison to the matrix. The mechanical properties, such as hardness and tensile strength, exhibited substantial enhancement relative to the A356 base alloy. Nonetheless, the elongation of the hybrid material under tensile stress decreased from 13.23% to 9.41%, indicating enhanced strength but reduced ductility. From the above literature various particles used to study the impact of dual particles addition on the mechanical behavior of Al alloy composites.

The primary objective of this research is to construct hybrid composites by including  $Al_2O_3$  particles with a size range of 25 microns and graphite particles with a consistent weight percentage of 5 microns. The objective of this study is to investigate the impact of different concentrations of  $Al_2O_3$  particles (ranging from 3 to 6 weight percent) and graphite particles (maintaining a constant 2 weight percent) on the mechanical behaviour and tensile fractography of Al2219 composites. Additionally, the study will examine the microstructure, mechanical properties, and wear parameters of the alloy.

## 2. Experimental Details

### 2.1 Matrix and Reinforcement Materials

The procurement of Al alloy Al2219 ingots from FENFE Metallurgical in Bengaluru, India, is intended solely for this purpose. The chemical composition of the Al2219 alloy used in the study is presented in Table 1. The  $Al_2O_3$  and graphite particles obtained from Bio-aid Scientific Industries Pvt. Ltd. in Bangalore, India were used as reinforcements. Their dimensions were 25  $\mu m$  and 5  $\mu m$ , respectively. Table 2 provides a comprehensive overview of the properties of the reinforcements and matrices. Fig. 1(a-b) illustrates the hybrid composites consisting of Al2219,  $Al_2O_3$ , and graphite. This is a scanning electron microscope image of the  $Al_2O_3$  and graphite particles that were utilised in the fabrication of the material.



(a)

(b)

Fig. 1. SEM micrographs of (a) 25-micron sized  $Al_2O_3$  particles (b) 5 micron sized graphite particles

Table 1. Chemistry of Al2219 alloy by wt. %

Si	Fe	Cu	Mn	Mg	Zn	Ti	Al
0.20	0.28	6.50	0.30	0.02	0.10	0.15	Balance

Table 2. Properties of Al2219 alloy, Al<sub>2</sub>O<sub>3</sub> and Graphite particles

Material	Hardness (BHN)	Density (g/cm <sup>3</sup> )	Elastic Modulus (GPa)	Tensile Strength (MPa)
Al2219	70	2.82	70	220
Al <sub>2</sub> O <sub>3</sub>	2700	3.96	400	325
Graphite	1.7*	2.20	16	160

\*Mohs hardness

## 2.2. Composite Fabrication

The sample was created using the conventional stir-casting procedure. Aluminium 2219, weighing one kilogramme, was melted in an electric furnace at a temperature of 700°C. The furnace contained a graphite crucible and was filled with argon gas. The purpose of this process was to generate composites. To produce the homogenised melt, the furnace was heated to a temperature of 750°C and kept at that level for a duration of 25 minutes. Continuous flow of heated graphite and alumina particles was added to the liquid metal. The reinforcement was thoroughly blended for 15 minutes at a speed of 500 revolutions per minute to provide uniform dispersion. Once the temperature of the cast-iron die had decreased to match that of the surrounding room, the slurry made from a combination of synthetic materials and aluminium was poured into it. An identical technique was utilised to fabricate Al2219 alloy composites including Al<sub>2</sub>O<sub>3</sub> particles in the range of 3 to 6 weight percent, while keeping the graphite particles at a constant 2 weight percent. Figure 2 (a-d) represents the furnace set up used for the study, cast iron die, casting in the cast iron die and a sample of casting with tensile specimen respectively. Various sample prepared for the study are detailed in Table 3.



(a)



(b)



Fig. 2. Showing the (a) Furnace set up (b) Cast iron die (c) Casting in die (d) Sample of casting and tensile test specimen

Table 3. List of various composites prepared

Sl. No.	Material Code	Compositions of composites prepared
1	A	As-cast Al2219 Alloy
2	C1	Al2219 + 3 wt.% Al <sub>2</sub> O <sub>3</sub> + 2 wt.% Graphite composites
3	C2	Al2219 + 6 wt.% Al <sub>2</sub> O <sub>3</sub> + 2 wt.% Graphite composites

### 2.3. Testing of Composites

The study's composite casting was meticulously polished using polishing materials with abrasive particles smaller than three microns at a low speed, after being disassembled into many pieces from various locations. Polishing was employed to eradicate the superficial abrasions from the composites. The final steps of the polishing procedure involved the use of emery sheets that contained abrasives made from SiC and Al<sub>2</sub>O<sub>3</sub>. In order to enhance the optical clarity, Kellar's reagent was employed, comprising of hydrochloric acid, hydrofluoric acid, nitric acid, and water. Once the surface was thoroughly cleaned and polished, cotton swabs saturated with etchant were employed to administer Kellar's reagent [19, 20]. Subsequently, the SEM pictures were generated by delicately rotating the surface to evenly distribute the reagent.

The ASTM D792 [21] approach use standard test pieces with a diameter of 12 mm and a length of 30 mm for density calculations. In order to determine the mass of the sample, we immerse it in distilled water at the ambient temperature and employ a digital balance with a precision of 0.001 g. The density of a composite can be empirically evaluated by employing a physical offset and calibrating the equipment in accordance with ASTM D792-66.

This investigation utilises a Brinell hardness tester that has been calibrated in accordance with the requirements outlined in ASTM E10 [22]. The Brinell test is generally required for surfaces that are excessively rough for standard testing equipment to handle. The hardness of both the as-cast and composited Al2219 alloy with Al<sub>2</sub>O<sub>3</sub> particles was measured using a 5 mm ball indenter. Different durations were employed to exert a force of 250 kgf on each sample. The tension test is conducted using a Universal Testing Machine (UTM) that complies with the standards set by ASTM E8 [23]. The sample is subjected to controlled circumstances and stretched until it fractures. This test provides crucial information, such as the metal's response to tensile stress. A tension test can determine the failure point of a material by subjecting it to a significant amount of tensile stress. This method simplifies the process of determining the safety factor of a material and its maximum load capacity



prior to failure. Furthermore, engineers can employ it to determine whether a material is suitable for a certain application. Specimens were subjected to uniaxial tensile testing following preparation according to ASTM E8 standards for tension testing. The specimen is 45 millimetres in length and has a diameter of 9 millimetres. The tensile test was performed using an Instron servo-hydraulic apparatus with a cross head speed of 0.28 mm/min. Composites undergo testing at normal room temperature conditions.

### 3. Results and Discussion

#### 3.1 Microstructural Analysis

The synthesised hybrid composites demonstrate a notable reduction in porosity, as observed in scanning electron micrographs of Al2219 mixed with Al<sub>2</sub>O<sub>3</sub> and graphite particles. Scanning electron microscopy was used to analyse composites containing varying quantities of Al<sub>2</sub>O<sub>3</sub> and a fixed proportion of graphite. Fig. 3 (a) displays the scanning electron microscope (SEM) photos of the pure Al2219 alloy. Fig. 3 (b) exhibits the same alloy with 3% Al<sub>2</sub>O<sub>3</sub> and 2% graphite reinforcement. Fig. 3 (c) showcases the same alloy with 6% Al<sub>2</sub>O<sub>3</sub> and 2% graphite reinforcement. These photographs provide a visual representation of the microstructure of these artificial aluminium hybrid composites.

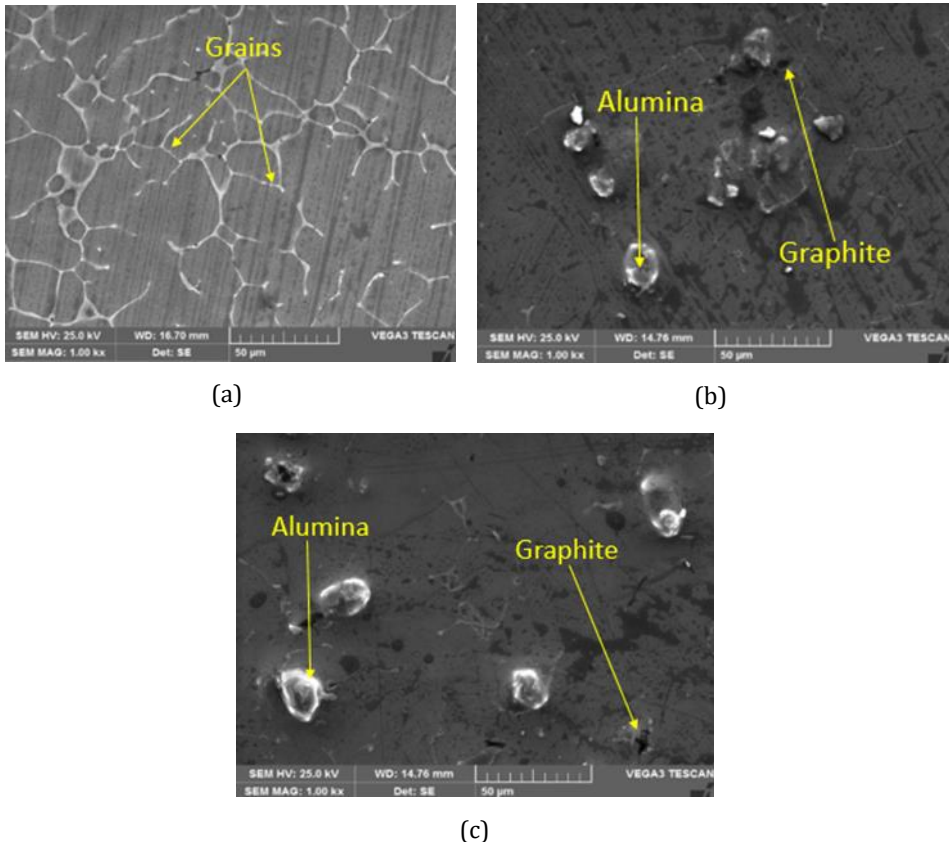
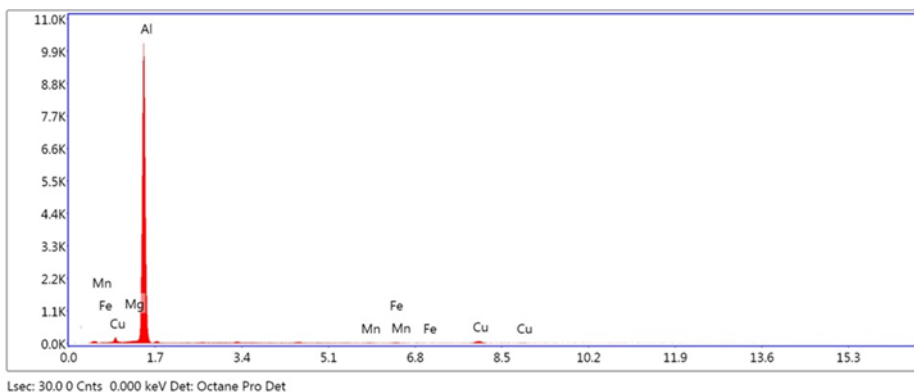


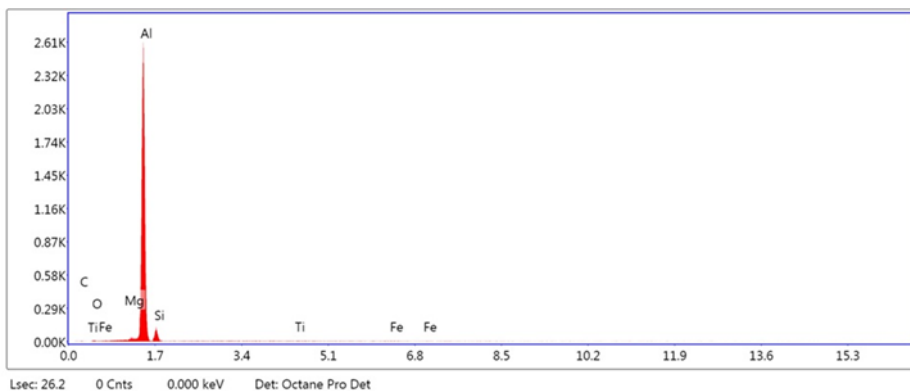
Fig. 3. SEM micrographs of (a) as-cast Al2219 alloy (b) Al2219 alloy with 3 wt. % of Al<sub>2</sub>O<sub>3</sub> and 2 wt. % of Graphite composite (c) Al2219 alloy with 6 wt. % of Al<sub>2</sub>O<sub>3</sub> and 2 wt. % of Graphite composite

Temperature differences between the solid matrix and the reinforcing particles help in the development of aluminium composites. Because ceramic particles have lower heat conductivity than the Al2219 melt, the molten matrix is at a higher temperature. During the development of dendrites in the first generation of Al2219 grains, the microstructure of the Al2219 silicate eutectic reveals the presence of an inter-dendritic zone between the Si and Al grains. The surface of Al-cast composites can be polished to achieve a highly reflective appearance. Increased magnification will allow for the observation of the grain boundary and secondary phases that are visible under a microscope (Fig. 3(a)). The properties of the composites are determined by the microstructure and features of the reinforcement-to-Al edge. Fig. 3(b-c) shows the scanning electron microstructures of MMCs reinforced with Al<sub>2</sub>O<sub>3</sub> and graphite. Microstructure examination did not provide any evidence of aggregated or grouped reinforcements in the MMCs. The causes for this were the continuous contact time between Al<sub>2</sub>O<sub>3</sub> and the graphite particle in the liquid Al during the production of the composites, as well as the circulation of the same reinforcement throughout the stirring process.

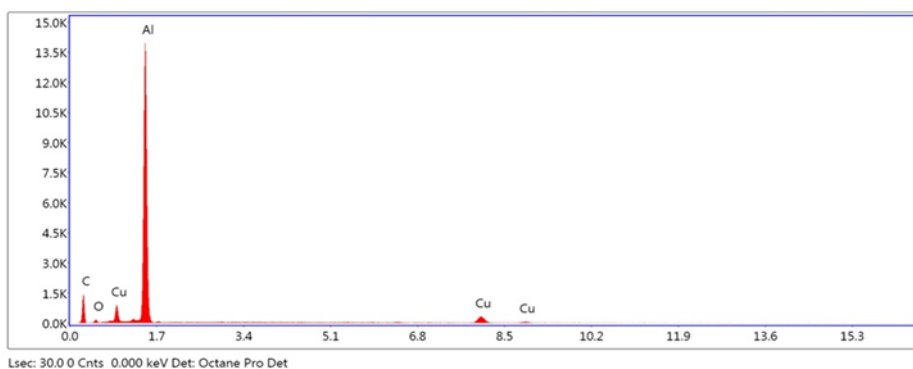
The reinforcing components seem to be uniformly distributed. The results and variable composition exhibited strong concordance, while the microstructure analysis of the composites had more limitations than those of the matrix alloy when all conditions were taken into account. In addition, the Al<sub>2</sub>O<sub>3</sub> and graphite are consistently dispersed throughout the aluminium matrix. The Gr particles maintain their polygonal shape as the quantity of Al<sub>2</sub>O<sub>3</sub> particles increases. However, Fig. 3 (c) demonstrates the aggregation of Al<sub>2</sub>O<sub>3</sub> particles in the composite region. The reinforcing components seem to be uniformly distributed. The results and variable composition exhibited a high level of concordance. However, when considering all conditions, the microstructure analysis of the composites imposed greater limitations compared to the matrix alloy. The Gr particles maintain their polygonal shape as the quantity of Al<sub>2</sub>O<sub>3</sub> particles increases; however, the aggregation of Al<sub>2</sub>O<sub>3</sub> particles in the composite region is depicted in Fig. 3 (c). By utilizing EDS, a pragmatic and efficient technique, it is possible to determine the comparative frequencies of constituents and confirm their existence. Chemical analysis can identify the composition of a sample, but quantifying the exact amount of each element can be challenging. The composite material depicted in Fig. 4 b and Fig. 4C consists of an Al2219 alloy combined with 3 and 6 wt.% Al<sub>2</sub>O<sub>3</sub> and 2 wt.% graphite. Si, Fe, Mg, Cu, and Zn are essential alloying elements in Al2219, as depicted in Fig. 4 (a). Fig. 4 (b and c) displays the EDS spectra of composites reinforced with 3 and 6 weight percent Al<sub>2</sub>O<sub>3</sub> particles, as well as a constant 2 weight percent graphite comprised of Al2219. Graphite and alumina particles include C and O elements as shown in the EDS composites spectra.



(a)



(b)



(c)

Fig. 4. EDS spectrums of (a) as-cast Al2219 alloy (b) Al2219 alloy with 3 wt. % of Al<sub>2</sub>O<sub>3</sub> and 2 wt. % of Graphite composite (c) Al2219 alloy with 6 wt. % of Al<sub>2</sub>O<sub>3</sub> and 2 wt. % of Graphite composite

### 3.2 Density Measurements

Fig. 5 displays the densities of three different materials: Al2219 aluminium alloy (A), Al2219 with 3% Al<sub>2</sub>O<sub>3</sub> and 2% graphite (C1), and Al2219 with 6% Al<sub>2</sub>O<sub>3</sub> and 2% graphite (C2) hybrid composites. The graph displays a comparison between the theoretical and experimental densities. A study has been conducted to investigate the impact of Al<sub>2</sub>O<sub>3</sub> and graphite particles on the Al2219 alloy. The cumulative impacts of these hybrid particles are illustrated in Fig. 5. The theoretical values computed using the standard rule of mixture exhibit a greater abundance of values compared to the experimental data. The density of aluminium alloy 2219 has been determined to be 2.80 g/cm<sup>3</sup>. The densities of the reinforcing components, Al<sub>2</sub>O<sub>3</sub> and Gr, are 3.96 g/cm<sup>3</sup> and 2.52 g/cm<sup>3</sup>, respectively. The graph demonstrates the Al2219—2% graphite and 6% Al<sub>2</sub>O<sub>3</sub> (C2) composites had lower densities when compared to the base matrix and other hybrid composites. The proximity between the predicted and experimental densities, as observed in Fig.5, suggests that the stir approach is a feasible technique for manufacturing hybrid composites. Several studies [24] have analysed the impact of Al<sub>2</sub>O<sub>3</sub> and Gr on the density of various Al alloys.



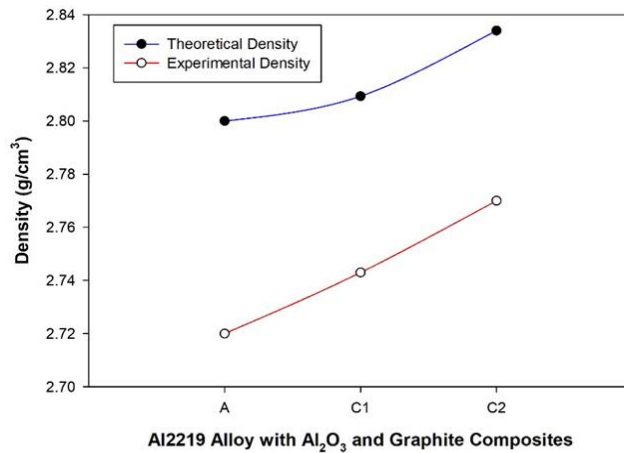


Fig. 5. Theoretical and experimental densities of Al2219 alloy and its Al<sub>2</sub>O<sub>3</sub>-Graphite composites

### 3.3 Hardness Measurements

Fig. 6 displays the hardness of the hybridised composites and the substrate metal Al2219. Composites that are reinforced exhibit a greater level of hardness compared to those that are not reinforced, and the level of hardness increases in proportion to the weight % of the reinforcement. This statement is accurate, as evidenced by the primary study sources [25, 26]. Incorporating robust reinforcing particles enhances the strength and toughness of the matrix. Due to the increased graphite content, the composites exhibit a larger percentage of softness in the 2 weight percent Gr and 3 weight percent Al<sub>2</sub>O<sub>3</sub> particles. Based on the graphs, increasing the amount of Al<sub>2</sub>O<sub>3</sub> in the matrix results in an enhancement of the hardness of the hybrid composite. The alloy's hardness was enhanced by including various proportions of Al<sub>2</sub>O<sub>3</sub>, which possesses greater hardness compared to most other materials. The improved hardness of hybrid composites may be attributed to the reduced porosity observed in scanning electron micrographs. Table 4 presents the hardness and standard deviation values for the Al2219 alloy and its hybrid composites.

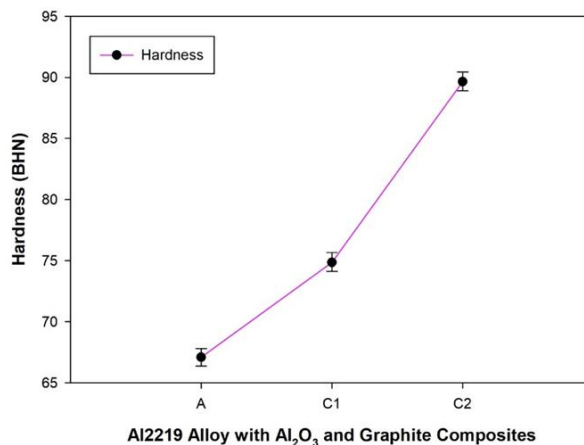


Fig. 6. Hardness of Al2219 and its Al<sub>2</sub>O<sub>3</sub>-graphite reinforced hybrid composites

The increased hardness value of the Al-Gr-Al<sub>2</sub>O<sub>3</sub> hybrid composite can be accredited to the uniform dispersion of Al<sub>2</sub>O<sub>3</sub> particles, which sets it apart from other made composites. The presence of fine Gr and hard Al<sub>2</sub>O<sub>3</sub> particles made grain boundary sliding more difficult. The addition of Al<sub>2</sub>O<sub>3</sub> to a composite enhances its hardness by elevating the dislocation density at the interfaces between the particles and the matrix. This phenomenon results from a disparity in thermal expansion between the matrix and the reinforcement. These components considerably limit the degree to which indentation induces localised deformation. Hardness testing revealed that the composites displayed enhanced hardness with an increase in the amount of Al<sub>2</sub>O<sub>3</sub> reinforcement. Additionally, Gr was incorporated into the mixture to enhance its lubricating properties. Furthermore, studies have demonstrated that the presence of a larger Al<sub>2</sub>O<sub>3</sub> component enhances the toughness of the material in comparison to a solid aluminium alloy. This is achieved by creating a barrier that hinders the movement of dislocations [27, 28].

### 3.4 Tensile Properties

Tensile testing of hybrid composites was performed at ambient temperature in accordance with the protocols specified in ASTM E-8. To reduce the margin of error, we used interpolation to determine the average value based on three sets of standard specimens. The data presented in Figures 7 and 8 clearly indicate that the synthetic composites exhibit higher tensile and yield strengths compared to the monolithic Al2219 alloy.

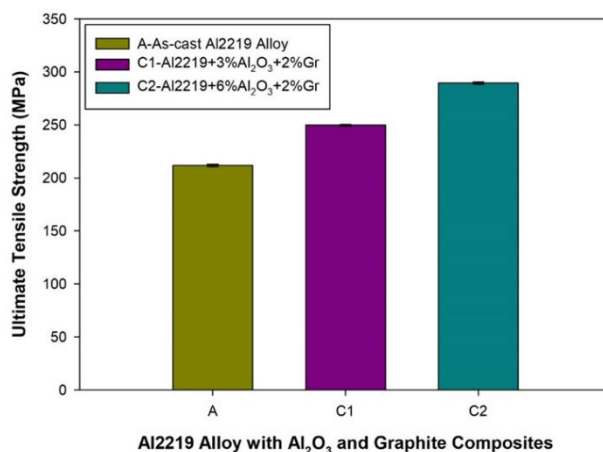


Fig. 7. Ultimate tensile strength of Al2219 with Al<sub>2</sub>O<sub>3</sub>-graphite reinforced hybrid composites

The microstructure encompasses the selection of the optimal grain size, the interfacial bonding between the Al2219 and reinforcement, and the uniform distribution of the reinforcement. Strain gradients play a role in strengthening composites. The recrystallization of Al2219 aluminium alloy is facilitated by the presence of a robust ceramic reinforcement, which serves as a site for nucleation. When a strengthened particle emerges from the nucleation process, it impedes the movement of the grain boundary, resulting in this occurrence. As a result, when compared to the Al2219 alloy without reinforcement, the size of the matrix grains is significantly larger. Grain boundaries play a dominant role in the movement of dislocations in artificial aluminium hybrid composites. The uninterrupted immobilisation of dislocations inside the matrix has resulted in a decrease in grain size [29]. This reduces the strengthening impact of dislocation movement in hybrid composites. The addition of Gr and Al<sub>2</sub>O<sub>3</sub> to an aluminium matrix alloy enhances the properties of the alloy, thereby impacting the results of the tensile test.

The high strength values of Al-Gr  $\text{Al}_2\text{O}_3$  hybrid composites can be accredited to the occurrence of dislocation pile-up, which arises from the existence of equally scattered  $\text{Al}_2\text{O}_3$  in the composite matrix. As the strength of the composite increases, both the density of dislocations and the density of dislocation interactions at matrix/reinforcement contacts also rise. The Hall-Petch relationship, which is dependent on the Gr particles, elucidates this phenomenon. The integration of  $\text{Al}_2\text{O}_3$  particles enhances the strength and ductility of typically brittle hybrid composites [30, 31].

The enhancements in the ultimate tensile strength (UTS) are achieved in the Al2219 matrix following reinforcement with rigid alumina particles. This improvement is attributed to the increased incorporation of alumina in the base Al2219, while maintaining a consistent graphite concentration. The matrix strength is enhanced by the inclusion of reinforcing particles, resulting in greater resistance to tensile stress. Moreover, due to the superior strength and rigidity of alumina particles compared to Al2219, these alumina and graphite particles initially endure significant stress with minimal deformation. The geometric constraints imposed by dual particles result in the inclusion of particles in the alloy, which enhances work hardening and hence improves tensile strength.

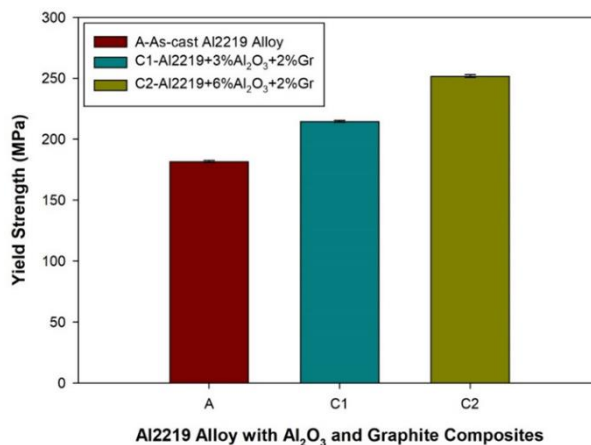


Fig. 8. Yield strength of Al2219 alloy and its  $\text{Al}_2\text{O}_3$  -graphite reinforced hybrid composites

The dislocation hypothesis elucidates the relationship between the size of particles and the tensile strength. The critical strain required for plastic deformation can be attributed to a significant quantity of dislocations that possess the ability to move freely. Dislocations at the grain boundary might collect and travel at a reduced velocity. Once the quantity of dislocations above a specific threshold, the movement of the dislocations will be driven by their content [32, 33]. The dislocation pile-up, size of  $\text{Al}_2\text{O}_3$  particles, and dislocation force all increase. Consequently, alloys that possess tiny grain sizes have significant strength. As the size of particles reduces, it becomes simpler to count the borders between particles, which in turn facilitates the prevention of dislocation migration. Hence, the dimensions of the Gr particles have a crucial role in determining the ultimate strength during plastic deformation [34, 35].

Fig. 9 demonstrates the impact of  $\text{Al}_2\text{O}_3$  and graphite reinforcement on the ductility of Al2219. The existence of rigid  $\text{Al}_2\text{O}_3$  particles has decreased the ductility in the Al2219. The addition of 3 weight percent  $\text{Al}_2\text{O}_3$  (C1) particles and 2 weight percent soft graphite particles to the Al2219 alloy results in a substantial enhancement of its ductility. Fig. 9 demonstrates that the composites with the smallest percentage of elongation were the

ones that had a composition of 2 weight percent graphite and Al2219-6 weight percent Al<sub>2</sub>O<sub>3</sub>. Other researchers who have examined these composites reinforced with particles have reached same findings. When hard, brittle particles are present, they impede deformation and reduce ductility [36, 37]. The primary cause of decreased elongation in the Al2219 matrix is the existence of hard and brittle particles.

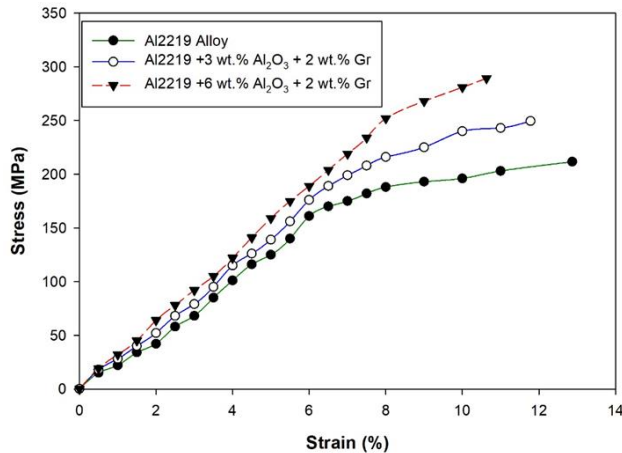


Fig. 9. Elongation of Al2219 alloy and its Al<sub>2</sub>O<sub>3</sub>-graphite reinforced hybrid composites

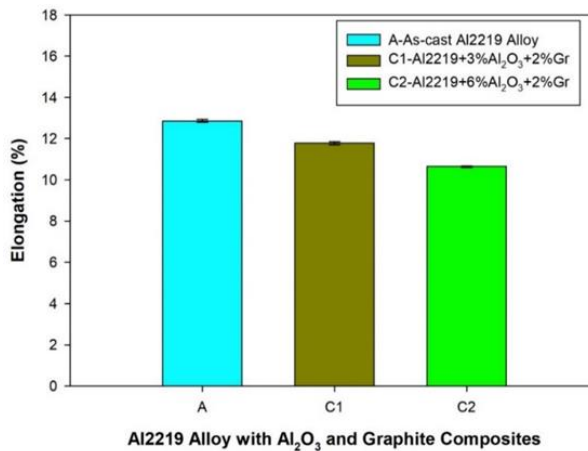


Fig. 10. Stress-strain plots of as-cast Al2219, Al2219 with 3 wt. % of Al<sub>2</sub>O<sub>3</sub> and 2 wt. % of Graphite composite and Al2219 with 6 wt. % of Al<sub>2</sub>O<sub>3</sub> and 2 wt. % of Graphite composite

The results demonstrate that the mechanical strength and tensile strength of Al2219 are improved by the inclusion of 3% graphite and 6% Al<sub>2</sub>O<sub>3</sub>. Fractures, perforations, and fractures are indications of brittle fracture. If the amounts of Gr particles remain constant and the concentration of Al<sub>2</sub>O<sub>3</sub> increases, the occurrence is more probable. The composites are exhibiting increased brittleness, as shown by the visible surface fracture and crack propagation. One potential reason is because the percentage of elongation reduces as the final tensile strength increases, as stated in reference [38]. Fig. 10 is showing the stress-strain plots of as cast alloy, Al2219 alloy with 2 wt.% of graphite and varying 3 and 6 wt.%

of alumina composites respectively. The resistance to deformation has been enhanced with the inclusion of particles.

### 3.5 Tensile Fractography

The tensile fracture surfaces of Al2219 alloy, Al2219-3 % Al<sub>2</sub>O<sub>3</sub>-2 % of graphite and Al2219 -6 % & Al<sub>2</sub>O<sub>3</sub>-2 % of graphite composites studied as shown in Fig. 11 (a-c). Fig. 11 (a) shows that the superficial of the Al sample cracks in a fibrous manner. Fig. 11 (b, c) displays the fractures in the Al2219 with a weight percentage of 3%. The composition consists of 2 weight percent graphite and 3 weight percent Al<sub>2</sub>O<sub>3</sub> in Al2219 alloy, and 6 weight percent Al<sub>2</sub>O<sub>3</sub> and 2 weight percent graphite in the same alloy. By incorporating rigid Al<sub>2</sub>O<sub>3</sub> particles into the matrix, the ductility of the material diminishes while its strength increases, resulting in enhanced stiffness and strength.

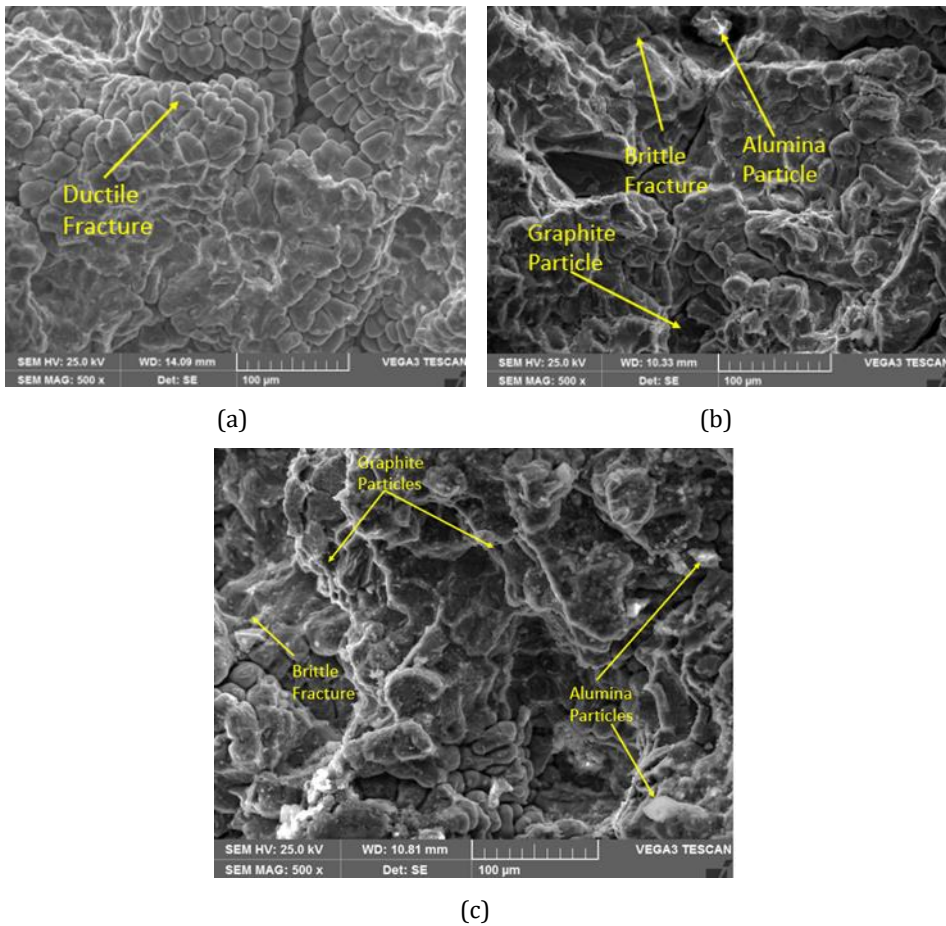


Fig. 11. Tensile fractured surfaces SEM images of (a) of (a) as-cast Al2219 (b) Al2219 with 3 wt. % of Al<sub>2</sub>O<sub>3</sub> and 2 wt. % of Graphite composite (c) Al2219 with 6 wt. % of Al<sub>2</sub>O<sub>3</sub> and 2 wt. % of Graphite composite

SEM micrographs of composite materials exhibit a combination of shear and brittle fracture modes. The varying sizes of the matrix dimples on the fracture surface can be observed in Fig. 11 (b, c). The inclusion of soft graphite in the matrix enhances the ductility

of composites. However, the presence of alumina particles diminishes this effect. SEM micrographs [39, 40] reveal that composites exhibit a fracture mode that is a combination of ductile and brittle behaviour, which is attributed to the combined influence of graphite and  $\text{Al}_2\text{O}_3$  particles.

#### 4. Conclusion

The current study examined the mechanical characteristics of composites reinforced with graphite and  $\text{Al}_2\text{O}_3$  particles manufactured of Al2219 matrix. The conclusions that followed were as follows:

- Using the stir cast method, hybrid composites of Al2219 with graphite and  $\text{Al}_2\text{O}_3$  reinforcement were created. Al2219 with 3 and 6 wt.% of  $\text{Al}_2\text{O}_3$  and constant 2 wt. % of graphite hybrid composites were studied.
- The scanning electron microscope images revealed a consistent distribution of  $\text{Al}_2\text{O}_3$  and graphite within the Al2219. The EDS spectra indicate the presence of Carbon and Oxygen in the composites of Al2219 with  $\text{Al}_2\text{O}_3$  and graphite.
- With an incorporation of alumina and graphite particles, the density of Al2219 alloy was increased. Al2219 composites containing 2% graphite and 6%  $\text{Al}_2\text{O}_3$  had the highest density. The hardest composites are made of Al2219 with 2% graphite and 6%  $\text{Al}_2\text{O}_3$ .
- Al2219 alloy hardness was increased with the addition of  $\text{Al}_2\text{O}_3$  and graphite. Al2219 with 6 wt.% of alumina and 2 wt. % of graphite composites exhibited highest hardness and improvement in the hardness was 33.6%.
- The ultimate and yield strengths of Al2219 were improved by using graphite and  $\text{Al}_2\text{O}_3$  reinforcements. The maximum ultimate and yield strength was recorded in the composites reinforced with 6 wt.% alumina and 2 wt.% graphite. The addition of  $\text{Al}_2\text{O}_3$  particles (6% by weight) and graphite (2% by weight) results in an increase of 36.7% in ultimate tensile strength (UTS) and 38.5% in yield strength (YS) of the Al2219 alloy.
- Graphite and  $\text{Al}_2\text{O}_3$  have slightly reduced the ductility of the Al2219 matrix. The impact of hard alumina particles on the ductility of Al2219 alloy was more and hence caused in the reduction of elongation.
- According to a surface microscopic investigation of tensile fractures, the as-cast Al2219 exhibits ductile fracture behaviour, while the hybrid composites containing  $\text{Al}_2\text{O}_3$  and graphite particles, displayed brittle fracture behaviour.

#### References

- [1] Bharath V, Nagaral M, Auradi V. Preparation of 6061Al- $\text{Al}_2\text{O}_3$  metal matrix composite by stir casting and evaluation of mechanical properties. International Journal of Metallurgical & Materials Science and Engineering, 2012;2 (3): 22-31.
- [2] Nagaral M, Auradi V, Kori SA. Microstructure and mechanical properties of Al6061-Graphite composites fabricated by stir casting process. Applied Mechanics and Materials, 2015;766: 308-314. <https://doi.org/10.4028/www.scientific.net/AMM.766-767.308>
- [3] Pankaj RJ, Sridhar BR, Nagaral M, Jayasheel IH, Evaluation of mechanical properties of B4C and graphite particulates reinforced A356 alloy hybrid composites, Materials Today: Proceedings, 2017; 4(9), 9972-9976. <https://doi.org/10.1016/j.matpr.2017.06.304>
- [4] Siddesh M, Shivakumar BP, Shashidhar S, Nagaral M. Dry sliding wear behavior of mica, fly ash and red mud particles reinforced Al7075 alloy hybrid metal matrix composites,



- Indian Journal of Science and Technology, 2021;14 (4): 310-318. <https://doi.org/10.17485/IJST/v14i4.2081>
- [5] Nagaral M, Hiremath V, Auradi V, Kori SA. Influence of Two-Stage Stir Casting Process on Mechanical Characterization and Wear Behavior of AA2014-ZrO<sub>2</sub> Nano-composites, Transactions of the Indian Institute of Metals, 2018; 71: 2845-2850. <https://doi.org/10.1007/s12666-018-1441-6>
- [6] Veeresh Kumar GB, Gude VC, Mandadi SV, Jayarami R, Nagaral M, Naresh K. Effects of addition of Titanium Diboride and Graphite Particulate Reinforcements on physical, mechanical and tribological properties of Al6061 Alloy based Hybrid Metal Matrix Composites, Advances in Materials and Processing Technologies, 2022; 8 (2), 2259-2276. <https://doi.org/10.1080/2374068X.2021.1904370>
- [7] Nagaral M, Attar S, Reddappa HN, Auradi V, Kumar S, Raghu S. Mechanical behavior of Al7025-B4C particulate reinforced composites. Journal of applied mechanical engineering, 2015; 4(6), 1-4.
- [8] Bharath V, Auradi V, Nagaral M, Satish BP. Experimental Investigations on Mechanical and Wear Behaviour of 2014Al-Al<sub>2</sub>O<sub>3</sub> Composites. Journal of Bio-and Tribo-Corrosion, 2020;6: 1-10. <https://doi.org/10.1007/s40735-020-00341-2>
- [9] Nagaral M, Auradi V, Parashivamurthy KI, Kori SA, Shivananda BK. Synthesis and characterization of Al6061-SiC-graphite composites fabricated by liquid metallurgy. Materials Today: Proceedings, 2018; 5(1): 2836-2843. <https://doi.org/10.1016/j.matpr.2018.01.073>
- [10] Nagaral M, Auradi V, Kori SA, Reddappa HN, Jayachandran, Veena S. Studies on 3 and 9 wt.% of B4C particulates reinforced Al7025 alloy composites. AIP conference proceedings, 2017;1:1859. <https://doi.org/10.1063/1.4990172>
- [11] Sallahuddin A, Madeva N, Reddappa HN, Auradi V. Effect of B4C particulates addition on wear properties of Al7025 alloy composites. American Journal of Materials Science, 2015;5(3C): 53-57.
- [12] Bharath V, Auradi V, Nagaral M, Satish BB, Ramesh S, Palanikumar K. Microstructural and wear behavior of Al2014-alumina composites with varying alumina content, Transactions of the Indian Institute of Metals, 2021;75: 133-147. <https://doi.org/10.1007/s12666-021-02405-4>
- [13] Vasanth Kumar HS, Kempaiah UN, Nagaral M, Revanna K. Investigations on mechanical behaviour of micro B4C particles reinforced Al6061 alloy metal composites. Indian Journal of Science and Technology, 2021; 14 (22): 1855-1863. <https://doi.org/10.17485/IJST/v14i22.736>
- [14] Nagaral M, Auradi V, Kori SA, Veena S. Mechanical characterization and wear behavior of nano TiO<sub>2</sub> particulates reinforced Al7075 alloy composites, Mechanics of Advanced Composite Structures, 2020; 7(1): 71-78.
- [15] Zeeshan A, Muthuraman V, Rathnakumar P, Gurusamy P, Nagaral M. Studies on mechanical properties of 3 wt% of 40 and 90 μm size B4C particulates reinforced A356 alloy composites. Materials Today: Proceedings, 2022;52: 494-499. <https://doi.org/10.1016/j.matpr.2021.09.260>
- [16] Raj Kumar, Deshpande RG, Gopinath B, Jayasheel H, Nagaral M, Auradi V. Mechanical Fractography and Worn Surface Analysis of Nanographite and ZrO<sub>2</sub>-Reinforced Al7075 Alloy Aerospace Metal Composites. Journal of Failure Analysis and Prevention, 2021; 21: 525-536. <https://doi.org/10.1007/s11668-020-01092-5>
- [17] V Bharath, Santhrusht S Ajawan, Madev Nagaral, Virupaxi Auradi, Shivaputrappa Amarappa Kori, Characterization and Mechanical Properties of 2014 Aluminum Alloy Reinforced with Al<sub>2</sub>O<sub>3</sub>p Composite Produced by Two-Stage Stir Casting Route, Journal of The Institution of Engineers (India): Series C, 100, 2019, 277-282. <https://doi.org/10.1007/s40032-018-0442-x>
- [18] Pathalinga GP, Chittappa HC, Nagaral M, Auradi V. Influence of B4C Reinforcement Particles with Varying Sizes on the Tensile Failure and Fractography of LM29 Alloy

- Composites, Journal of Failure Analysis and Prevention, 2020;20 (6): 2078-2086. <https://doi.org/10.1007/s11668-020-01021-6>
- [19] Zeeshan A, Muthuraman V, Rathnakumar P, Gurusamy P, Nagaral M. Investigation on the tribological properties of copper alloy reinforced with Gr/ZrO<sub>2</sub> particulates by stir casting route. Materials Today: Proceedings, 2020; 33: 3449-3453. <https://doi.org/10.1016/j.matpr.2020.05.351>
- [20] Nagaral M, Auradi V, Parashivamurthy KI, Kori SA. Wear behavior of Al<sub>2</sub>O<sub>3</sub> and graphite particulates reinforced Al6061 alloy hybrid composites. American Journal of Materials Science, 2015; 5 (3C): 25-29.
- [21] Samuel D, Satish BB, Virupaxi A, Nagaral M, Udaya MR, Bharath V. Evaluation of Wear Properties of Heat-Treated Al-AlB<sub>2</sub> in-situ Metal Matrix Composites, Journal of Bio-and Tribo-Corrosion, 2021;7,(40): 1-11. <https://doi.org/10.1007/s40735-021-00476-w>
- [22] Nagaraj N, Mahendra KV, Nagaral M. Microstructure and evaluation of mechanical properties of Al-7Si-fly ash composites, Materials Today: Proceedings, 2018; 5 (1): 3109-3116. <https://doi.org/10.1016/j.matpr.2018.01.116>
- [23] Nagaral M, Shivananda BK, Virupaxi A, Kori SA. Development and mechanical-wear characterization of Al<sub>2</sub>O<sub>3</sub>-nano B<sub>4</sub>C composites for aerospace applications, Strength, Fracture and Complexity, 2020;13 (1); 1-13. <https://doi.org/10.3233/SFC-190248>
- [24] Nagaral M, Shivananda BK, Auradi V, Parashivamurthy KI, Kori SA. Mechanical behavior of Al6061-Al<sub>2</sub>O<sub>3</sub> and Al6061-graphite composites, Materials Today: Proceedings, 2017; 4(10): 10978-10986. <https://doi.org/10.1016/j.matpr.2017.08.055>
- [25] Fazil N, Venkataramana V, Nagaral M, Auradi V. Synthesis and mechanical characterization of micro B<sub>4</sub>C particulates reinforced AA2124 alloy composites, International Journal of Engineering and Technology UAE, 2018; 7 (2.23): 225-229. <https://doi.org/10.14419/ijet.v7i2.23.11954>
- [26] Krishna D, Prashanth L, Nagaral M, Mathapati R, Hanumantharayagouda MB. Microstructure and mechanical behavior of B<sub>4</sub>C particulates reinforced ZA27 alloy composites, Materials Today: Proceedings, 2017;4,8: 7546-7553. <https://doi.org/10.1016/j.matpr.2017.07.086>
- [27] Veerabhadrapa A, Poornima H, Loksha V, Nagaral M, Auradi V. Machine learning algorithms to predict wear behavior of modified ZA-27 alloy under varying operating parameters, Journal of Bio-and Tribo-Corrosion, 2022; 8: 1-10. <https://doi.org/10.1007/s40735-021-00610-8>
- [28] Balaraj V, Nagaraj K, Nagaral M, Auradi V. Microstructural evolution and mechanical characterization of micro Al<sub>2</sub>O<sub>3</sub> particles reinforced Al6061 alloy metal composites, Materials Today: Proceedings, 2021; 47: 5959-5965. <https://doi.org/10.1016/j.matpr.2021.04.500>
- [29] Varadaraj KR, Kumar S, Vitala HR, Ravishankar MK, Dileep BP. Effect of Chromium on Mechanical and Corrosion Behaviour of Ferrous Metal Matrix Composites by Using Powder Metallurgy Route, Lecture Notes in Mechanical Engineering, 2023: 225-234. [https://doi.org/10.1007/978-981-19-4140-5\\_19](https://doi.org/10.1007/978-981-19-4140-5_19)
- [30] Sundararaj CP, Math MM, Girisha, Annigeri AR, Dileep BP. Machinability Study of Multilayer Coated Tungsten Carbide Inserts Using Chemical Vapor Deposition Techniques, Journal of The Institution of Engineers (India): Series D, 2023. <https://doi.org/10.1007/s40033-023-00604-5>
- [31] Anjan Kumar, Hanumantharayappa B, Chaithra P, Chethana CR, Chandrasekhar SB, Latha SB, Nagaral M, Suresh R. Synthesis and mechanical characterization of Si<sub>3</sub>N<sub>4</sub> reinforced copper-tin matrix composites. Journal of the Mechanical Behavior of Materials, 2021;30 (1): 199-206. <https://doi.org/10.1515/jmbm-2021-0020>
- [32] Bharath V, Auradi V, Nagaral M, Satish BB. Influence of alumina percentage on microstructure, mechanical and wear behavior of 2014 aluminium alumina metal matrix composites, Jurnal Tribologi, 2020;25 (1): 29-44.

- [33] Krishna SP, Samuel D, Rajesh M, Nagaral M, Auradi V, Rabin S. Preparation and mechanical characterization of TiC particles reinforced Al7075 alloy composites, *Advances in Materials Science and Engineering*, 2022: 7105189. <https://doi.org/10.1155/2022/7105189>
- [34] Pankaj RJ, Nagaral M, Shivakumar R, Jayasheel IH. Impact of boron carbide and graphite dual particulates addition on wear behavior of A356 alloy metal matrix composites, *Journal of Metals, Materials and Minerals*, 2020;30 (4): 106-112. <https://doi.org/10.55713/jmmm.v30i4.642>
- [35] Bharath V, Auradi V, Veeresh Kumar GB, Nagaral M, Chavali M, Mahmoud H, Rokayya S, Aljuraide, Jong WH, Ahmed MG. Microstructural Evolution, Tensile Failure, Fatigue Behavior and Wear Properties of Al2O3 Reinforced Al2014 Alloy T6 Heat Treated Metal Composites, *Materials*, 2022: 15 (12): 4244. <https://doi.org/10.3390/ma15124244>
- [36] Xie H, Fouad Y, Dileep BP, Kumar RS, Kannan S. Fabrication of high-performance LaFeO3/CuCo2O4 nanocomposite for X-band stealth application *Colloids and Surfaces A: Physicochemical and Engineering Aspects*, 2023; 677:132414. <https://doi.org/10.1016/j.colsurfa.2023.132414>
- [37] Vasanth Kumar HS, Kempaiah UN, Nagaral M, Auradi V. Impact, tensile and fatigue failure analysis of boron carbide particles reinforced Al-Mg-Si (Al6061) alloy composites, *Journal of Failure Analysis and Prevention*, 2021;21 (6): 2177-2189. <https://doi.org/10.1007/s11668-021-01265-w>
- [38] Nagaral M, Auradi V, Parashivamurthy KI, Shivananda BK, Kori SA. Dry sliding wear behaviour of aluminium 6061-SiC-graphite particulates reinforced hybrid composites, *IOP Conference Series: Materials Science and Engineering*, 2018;310: 012156. <https://doi.org/10.1088/1757-899X/310/1/012156>
- [39] Bharath V, Auradi V, Nagaral M. Fractographic characterization of Al2O3p particulates reinforced Al2014 alloy composites subjected to tensile loading, *Frattura ed Integrità Strutturale*, 2021;15(57): 14-23. <https://doi.org/10.3221/IGF-ESIS.57.02>
- [40] Nagaraj N, Mahendra KV, Nagaral M. Investigations on mechanical behaviour of micro graphite particulates reinforced Al-7Si alloy composites, *IOP conference series: materials science and engineering*, 2018; 310(1): 012131. <https://doi.org/10.1088/1757-899X/310/1/012131>
- [41] Bharath V, Ashita DH, Auradi V, Nagaral M. Influence of variable particle size reinforcement on mechanical and wear properties of alumina reinforced 2014Al alloy particulate composite, *FME Transactions*, 2020;48 (4), 968-978. <https://doi.org/10.5937/fme2004968B>
- [42] Paulo Davim J. *Metal Matrix Composites*, Materials, Manufacturing and Engineering, De Gruyter, 2014. <https://doi.org/10.1515/9783110315448>
- [43] Paulo Davim J. *Modern Mechanical Engineering*, Springer Publications 2014. <https://doi.org/10.1007/978-3-642-45176-8>
- [44] Kumar R, Deshpande RG, Shilpa RS, Rao KN, Nagaral M. Investigations on Mechanical Behavior of B4C and Graphite Particles Reinforced Al2117 Alloy Hybrid Metal Composites. *PalArch's Journal of Archaeology of Egypt/Egyptology*, 2021;17(6): 8052-8062.
- [45] Raksha MS et al. Impact of micro graphite particles addition on the mechanical behavior of Al2011 alloy metal composites. *Engineering Reports*, 2023;6(2): 1-10. <https://doi.org/10.1002/eng2.12746>
- [46] Pankaj Jadhav, Sridhar BR, Nagaraj M, Harti JI. Mechanical behavior and fractography of graphite and boron carbide particulates reinforced A356 alloy hybrid metal matrix composites. *Advanced Composites and Hybrid Materials*, 2020;3(1):114-119. <https://doi.org/10.1007/s42114-020-00143-7>